

Dynamic simulation of the effect of time-dependent variation of pH on response variable of the tailing thickener of coal washing plant

Mehdi Rahimi¹ · Ali Akbar Abdollahzadeh² · Bahram Rezaei¹

Received: 6 September 2018 / Revised: 3 February 2019 / Accepted: 14 February 2019 / Published online: 28 February 2019
© The Author(s) 2019

Abstract Dynamic simulation approach can be used for understanding the nonlinear behavior in mineral processing circuits. In this study, the gel point, the main parameters of batch flux density function and the main parameters of effective solid stress were determined at different conditions (pH, flocculant dosage and particle size). Therefore, the main parameters of phenomenological model of sedimentation and thickening were determined as a function of particle size, pH and flocculant dosages using the result of experimental tests and Curve expert professional software. Then, the dynamic simulation was carried out for the industrial thickener of coal washing plant and the time-dependent variation of response variables was investigated by time-dependent variation of pH of input feed to thickener using the obtained equations. It was observed that it is possible to predict the thickener behavior as a function of time for time dependent variation of pH of input feed to the thickener of coal washing plant using obtained equations that it was not possible using phenomenological model of thickener alone.

Keywords Dynamic simulation · Dewatering · Ideal continuous thickener · Thickener behavior · Time-dependent variation of pH

1 Introduction

In the mineral processing industries, the tailing material should be dewatered. During thickener operation, it is often desired to achieve certain amount of solid percent at the thickener underflow.

Sedimentation and thickening of flocculated suspension has attracted the attention of many researchers (Burger and Concha 1998). Many models have been developed by many researchers to simulate industrial thickeners.

Buscall and White (1987) presented the equation of effective solid stress as a function of solid volume fraction.

The effective solid stress ($\sigma_e(\phi)$) represents the stress in the compression zone. The equation of effective solid stress as a function of solid volume fraction and measurement of its parameters will be presented in the next section.

Landman et al. (1988) and Landman and White (1994) developed consolidation equations in the thickener with considering equation of effective solid stress as a function of solid volume fraction, critical solid volume fraction or gel point and hindered settling. These equations can be only used for prediction of thickener behavior in the steady state condition. They concluded that the required bed height to achieve the certain amount of solid percent at the thickener underflow is a function of effective solid stress, flux density function and cross section area of the thickener.

Burger and Concha (1998), Burger et al. (1999) and Garrido et al. (2004) proposed the phenomenological model for the sedimentation and thickening process by considering several constitutive assumptions. This theory allows the incorporation of compression/consolidation

✉ Mehdi Rahimi
rahimi.mehdi@yahoo.com

¹ Department of Mining and Metallurgical Engineering, Amirkabir University of Technology, Tehran, Iran

² Department of Mining Engineering, University of Kashan, Kashan, Iran

effects to the thickener modeling which was unavailable previously due to the non-existence/insignificance of bed/sediment inside conventional thickeners. These researchers considered the effect of effective solid stress, solid volume fraction at the beginning of compressive zone and hindered settling for design and simulation of a continuous thickener. The previous models that were proposed by the other investigators, could consider only steady state condition but the proposed model by these researchers is a dynamic model that can simulate the thickener performance at all times.

In the recent work, Barth et al. (2016) investigated the effect of uncertainty quantification for nonlinear hyperbolic problems with several random perturbations. In this research, feed concentration exhibits stochastic variability and feed flow rate is random perturbation.

Usher and Scales (2005) developed an algorithm to predict the bed height and solid volume fraction of discharge at steady state condition from fundamental material properties include the compressive yield stress ($P_y(\varphi)$) and the hindered settling function ($R(\varphi)$). Required input parameters of model are $P_y(\varphi)$, $R(\varphi)$ and thickener diameter as a function of thickener height, solid density, liquid density and solid volume fraction of feed.

Usher et al. (2009) developed the suspension dewatering equations based on aggregate densification. They presented the model for measurement of size distribution of aggregates. In this model, the shape of the aggregates is spherical and medium diameter is d . Settling rates were determined for different medium diameters of aggregates. They concluded that when the aggregates decrease in size, the tortuosities around the aggregates will decrease that lead to significant net decrease in the resistance to fluid flow. Therefore, they concluded that the settling rate will increase with decrease in aggregate size and increase in the density of these aggregates.

The presented model by Usher et al. (2009), assumed the aggregates had evolved to a final densified steady state before entering the consolidation zone of the thickener. However, densification and the associated evolution of the aggregate diameter which both depend on the solids residence time can occur throughout the consolidating bed in industrial thickeners. As densification occurs throughout the consolidation zone, both the solids volume fraction within the aggregates, φ_{agg} and the suspension gel point, φ_g , which can affect the sludge rheological properties, increase with the decrease of the aggregate diameter. The effects of densification as it occurs throughout the consolidating bed upon the sludge rheological properties must therefore be simulated and explored (Zhang et al. 2013).

Gladman et al. (2010) investigated the validation of the presented model by Usher. They validated the model by operating a pilot column continuously and measuring the

underflow solids. They confirmed that this model was the most accurate at the shortest residence times and lowest bed heights, but less accurate for longer residence times and higher beds. This was due to the changes in the dewatering properties of flocculated aggregates over time, which had not been adequately considered in the model.

Van Deventer et al. (2011) used the aggregate densification theory to predict the final equilibrium bed height by densification rate and bed compression. They also presented an equation between reduction of aggregate diameter and the thickening time. These researchers presented an equation for the densification rate, which provides the evolution of the aggregate diameters. An important parameter used in this equation is the aggregate densification rate parameter (A), which determines the required time to reach the final aggregate diameter in the steady state conditions. The aggregate densification rate parameter (A) also affects the rate of change of gel point (The solid volume fraction at the beginning of compressive zone) and the rate of change of solid volume fraction in aggregates. Therefore, in order to simulate and calculate the rheological parameters in the presence of densification, the aggregate densification rate parameter (A) should be considered that this parameter was not considered by Usher et al. (2009).

Zhou et al. (2014) used the residence-time distribution (RTD) and the compartment model to determine the flow regions in red mud separation thickener's feedwells. Their results showed that the inlet feed rate and the aspect ratio of feedwells are the most important parameters that affect the residence time distribution (RTD) of feedwell. Their results also showed that the volume fraction of dead zone can reduce by 10.8% and mixing flow volume fraction can increase 6.5% under the optimal operation conditions.

Rahimi et al. (2015) investigated the effect of pH, flocculant dosage and particle size on gel point and effective solid stress parameters of coal flotation tailing. In that research, the gel point and effective solid stress was measured using different batch settling and batch centrifuge tests, respectively. The results showed that in the case of nonfloculated suspension, the gel point increased with decreasing of pH, however, in the case of flocculated suspension the gel point decreased with decreasing of pH. The gel point also increased with increasing flocculant dosage in certain pH values for the two flocculated and nonfloculated fractions. In the case of nonfloculated suspension, the gel points for two different particle sizes were equal at a certain pH value but in the case of the flocculated suspension the gel point was higher for larger particle size. Likewise, the results showed that effective solid stress decreased with increasing gel point and settling rate.

Rahimi et al. (2017) numerically simulated the pilot thickener operation of copper mine using the phenomenological model and also validated the results for continuous and discontinuous tests. The continuous tests were performed in the plexiglass pilot thickener at different feed flow rates and discharge rates and the solid volume fraction of discharge, the bed height and the time were recorded for each condition. These tests were also simulated and it was observed that there is a good agreement between the results of continuous tests and the results of dynamic simulation. Secondly, the discontinuous tests were performed in the mentioned thickener at different feed flow rates with a discharge rate of zero. The bed formation rate was determined for each condition. These tests were also simulated and it was observed that there is a good agreement between the results of discontinuous tests and the results of simulation.

It was observed that many works have been done in the field of sedimentation and thickening process and many models have been presented for prediction of thickener behavior. Many of presented models can be used for prediction of thickener behavior at the steady state conditions (Landman et al. 1988; Usher and Scales 2005). The presented model by Burger et al. (1999) is a powerful model that can be used for dynamic simulation of thickeners at all time but it is not possible to simulate the time dependent variation of input pulp properties such as pH and flocculant dosage, time dependent variation of ore properties such as particle size of input feed to thickener using this model. In this paper, main parameters of proposed model by Burger et al. (such as gel point, batch flux density function and effective solid stress) are determined as a function of pH, flocculant dosage and particle size of input feed to thickener. Therefore, it is possible to simulate the behavior of industrial thickener for time-dependent variation of pH, flocculant dosage and particle size of input to thickener using obtained equations. The purpose of this research is dynamic simulation of the effect of time-dependent variation of pH on response variable (solid volume fraction of discharge and bed height) of the tailing thickener of coal washing plant that has not been investigated by the other investigators.

2 Phenomenological model of thickening and discretization

2.1 Phenomenological model of sedimentation and thickening

Burger and Concha (1998), Burger et al. (1999) and Garrido et al. (2004) presented the following field equation for

the solid volume fraction (φ) in the thickener as a function of height $0 \leq z \leq L$ and time $0 \leq t \leq T$:

$$\frac{\partial \varphi}{\partial t} + \frac{\partial}{\partial z} (q(t)\varphi + f_{bk}(\varphi)) = -\frac{\partial}{\partial z} (f_{bk}(\varphi) \frac{\sigma'_e(\varphi)}{\Delta \rho g \varphi} \frac{\partial \varphi}{\partial z}) \quad (1)$$

where φ is the solid volume fraction, z is the thickener height, $\Delta \rho$ is the solid–fluid density difference and g is acceleration of gravity. In the Eq. (1), we have:

$$q = (Q_D/S) \leq 0$$

where Q_D is the volumetric discharge rate and S is the cross-sectional area of the thickener.

In Eq. (1), $f_{bk}(\varphi)$ is the batch flux density function. ($f_{bk}(\varphi) < 0$). It is usually assumed that $f_{bk}(\varphi) = 0$ for $\varphi = 0$ and $\varphi = 1$ and $f_{bk}(\varphi) < 0$ for $0 < \varphi < 1$. A typical semi-empirical constitutive equation is given by the Richardson and Zaki (1954):

$$f_{bk}(\varphi) = u_\infty \varphi^a (1 - \varphi)^b \quad (2)$$

where parameters a and b are the constant parameters that are obtained using experimental tests and u_∞ represents the settling velocity of a single particle in unbounded fluid. For a particle of small diameter d , the velocity u_∞ is usually assumed to be given by the Stokes formula.

$$u_\infty = -\frac{\Delta \rho g d^2}{18 \mu_f} \quad (3)$$

where $\Delta \rho$ is the solid–fluid density difference, g is acceleration of gravity and μ_f is the dynamic viscosity of the pure fluid.

In Eq. (1), we have:

$$\sigma'_e(\varphi) = \frac{d\sigma_e(\varphi)}{d\varphi} \begin{cases} = 0 & \text{for } \varphi \leq \varphi_c \\ > 0 & \text{for } \varphi > \varphi_c \end{cases} \quad (4)$$

where $\sigma_e(\varphi)$ is the effective solid stress and φ_c is the critical solid volume fraction or gel point. The critical solid volume fraction (φ_c) or gel point is the solid volume fraction at the beginning of the compression zone and is the lowest volume fraction that flocs begin to touch each other. By increasing the pressure, the solid volume fraction increases. The effective solid stress ($\sigma_e(\varphi)$) which represents the stress in the compression zone is the stress which must be exceeded by an applied stress before the consolidation will occur. Buscall and White (1987) suggested that the effective solid stress, $\sigma_e(\varphi)$, is a function of the solid volume fraction, φ , and can be obtained through using Eq. (5):

$$\sigma_e(\varphi) = \sigma_0 ((\varphi/\varphi_c)^n - 1) \quad (5)$$

where parameters σ_0 and n are the constant parameters that are obtained using experimental tests and φ_c is the critical solid volume fraction or gel point. Equation (1) is a second

order quasilinear parabolic partial differential equation degenerating into first order hyperbolic type for the interval of solution values $[0, \varphi_c]$. Equation (1) does not have an analytical solution, but can be solved numerically using a finite difference method. The following initial conditions for solving degenerate parabolic partial differential equation (PDE) should be determined:

$$\varphi(z, 0) = \varphi_0(z) \quad 0 \leq z \leq L \tag{6}$$

$$\varphi(L, t) = \varphi_1(t) \quad 0 \leq t \leq T \tag{7}$$

The boundary conditions at $z = 0$ and $z = L$ for solving the degenerate parabolic partial differential equation (PDE) are as follows:

$$f_{bk}(\varphi(0, t)) \left(1 + \frac{\sigma'_e(\varphi(0, t))}{\Delta \rho g} \frac{\partial \varphi}{\partial z}(0, t) \right) = 0 \tag{8}$$

$$\begin{aligned} \frac{Q_D(t)}{S} \varphi(L, t) + f_{bk}(\varphi(L, t)) \left(1 + \frac{\sigma'_e(\varphi(L, t))}{\Delta \rho g} \frac{\partial \varphi}{\partial z}(L, t) \right) \\ = \frac{Q_F \varphi_F}{S} \end{aligned} \tag{9}$$

where Q_F is the feed flow rate, φ_F is the solid volume fraction of the thickener feed and Q_D is the volumetric discharge rate

2.2 Discretization

As mentioned before, Eq. (1) is complicated and does not have an analytical solution, but can be solved numerically using the finite difference method. PDE is discretized such that the entire thickener is modelled as a number of vertical sections (cells) with the height of $\Delta x = L/J$ and $\Delta t = T/N$, where J and N are integers representing the number of cells and number of time-steps respectively. Let φ_j^n denote the approximate value of φ at (x_j, t_n) where $x_j = j\Delta x$, $t_n = n\Delta t$. With assuming initial conditions φ_j^0 for $j = 0, 1, 2, \dots, J$, the discretized Eq. (1) is as follows:

$$\begin{aligned} \varphi_j^{n+1} = \varphi_j^n - \frac{1}{S_j} \left\{ \frac{\Delta t}{\Delta x} \left[Q_D(t_n) (\varphi_{j+1}^n - \varphi_j^n) \right. \right. \\ \left. \left. + S_{j+\frac{1}{2}} f_{bk}^{EO}(\varphi_j^n, \varphi_{j+1}^n) - S_{j-\frac{1}{2}} f_{bk}^{EO}(\varphi_{j-1}^n, \varphi_j^n) \right] \right. \\ \left. - \frac{\Delta t}{\Delta x^2} \left[S_{j+\frac{1}{2}} (A(\varphi_{j+1}^n) - A(\varphi_j^n)) \right. \right. \\ \left. \left. - S_{j-\frac{1}{2}} (A(\varphi_j^n) - A(\varphi_{j-1}^n)) \right] \right\} \end{aligned} \tag{10}$$

where

$$S_{j+1/2} = (S_j + S_{j+1})/2 \tag{11}$$

$$a(\varphi) = -\frac{f_{bk}(\varphi)\sigma'_e(\varphi)}{\Delta \rho g \varphi}, \quad A(\varphi) = \int_0^\varphi a(s) ds \tag{12}$$

$$\begin{aligned} f_{bk}^{EO}(\varphi_j, \varphi_{j+1}) = f_{bk}(0) + \int_0^{\varphi_j} \max\{f'_{bk}(s), 0\} ds \\ + \int_0^{\varphi_{j+1}} \min\{f'_{bk}(s), 0\} ds \end{aligned} \tag{13}$$

$$f_{bk}^{EO}(\varphi_j, \varphi_{j+1}) = \begin{cases} \varphi_{j+1} & \text{if } \varphi_j \leq \varphi_m \text{ and } \varphi_{j+1} \leq \varphi_m \\ \varphi_j + \varphi_{j+1} - \varphi_m & \text{if } \varphi_j > \varphi_m \text{ and } \varphi_{j+1} \leq \varphi_m \\ \varphi_m & \text{if } \varphi_j \leq \varphi_m \text{ and } \varphi_{j+1} > \varphi_m \\ \varphi_j & \text{if } \varphi_j > \varphi_m \text{ and } \varphi_{j+1} > \varphi_m \end{cases} \tag{14}$$

Incorporating the approximated boundary conditions given in Eqs. (8) and (9), the process descriptions in the discharge ($j = 0$) and feed ($j = J$) are given as follows:

$$\begin{aligned} \varphi_0^{n+1} = \varphi_0^n - \frac{1}{S_0} \left\{ \frac{\Delta t}{\Delta x} \left[Q_D(t_n) (\varphi_1^n - \varphi_0^n) + S_{\frac{1}{2}} f_{bk}^{EO}(\varphi_0^n, \varphi_1^n) \right] \right. \\ \left. - \frac{\Delta t}{\Delta x^2} \left[S_{\frac{1}{2}} (A(\varphi_1^n) - A(\varphi_0^n)) \right] \right\} \end{aligned} \tag{15}$$

$$\begin{aligned} \varphi_J^{n+1} = \varphi_J^n - \frac{1}{S_J} \left\{ \frac{\Delta t}{\Delta x} \left[Q_F(t_n) \varphi_F(t_n) - Q_D(t_n) \varphi_J^n \right. \right. \\ \left. \left. - S_{J-\frac{1}{2}} f_{bk}^{EO}(\varphi_{j-1}^n, \varphi_J^n) \right] + \frac{\Delta t}{\Delta x^2} S_{J-\frac{1}{2}} (A(\varphi_J^n) - A(\varphi_{j-1}^n)) \right\} \end{aligned} \tag{16}$$

To ensure the convergence of the resulting scheme, the following stability criterion must be satisfied:

$$\frac{1}{S_{min}} \left[\frac{\Delta t}{\Delta x} (\max|Q_D(t)| + S_{max} \max|f'_{bk}(\varphi)|) + \frac{2 \max a(\varphi) \Delta t}{\Delta x^2} \right] \leq 1 \tag{17}$$

3 Materials and methods

3.1 Material

The representative sample was obtained from the thickener feed (flotation tailing) of Tabas coal washing plant in south Khorasan province of Iran. Chemical and mineralogical analyses were performed by X-ray fluorescence (XRF) spectrometry and X-ray diffraction (XRD). According to these results, the main minerals of the sample are: Kaolinite, Quartz, Illite and Montmorillonite.

Sieve analysis for this sample was done and these results were obtained:

$$(d_{100})_1 = 500 \mu\text{m}, \quad (d_{80})_1 = 275 \mu\text{m}, \quad (d_{50})_1 = 70 \mu\text{m}$$

3.2 Determination of gel point, effective solid stress and batch flux density function as a function of pH, flocculant dosage and particle size

As mentioned in the Sect. 2, the effective solid stress, $\sigma_e(\phi)$, is a function of the solid volume fraction, ϕ , and can be obtained through using Eq. (5).

Experimental methods for measurement of the parameters σ_0 and n and also critical solid volume fraction (gel point) have been explained by Rahimi et al. (2015) and these parameters were determined at different conditions (pH, flocculant dosage and particle size).

According to experimental tests and using Curve expert professional software, parameters σ_0 , n and critical solid volume fraction (ϕ_c) were determined as a function of pH, flocculant dosage and particle size that are as follows:

$$n = 2.35 - (1.103 \times d_{80}) - (0.036 \times F) - (0.0231 \times \text{pH}) + (0.352 \times d_{80} \times F) + (0.00304 \times d_{80} \times \text{pH}) + (0.00219 \times F \times \text{pH}) + (0.00712 \times d_{80} \times F \times \text{pH}) \tag{18}$$

$$r^2 = 0.9687$$

$$\sigma_0 = -93982.6 - (1084798 \times d_{80}) - (16.6 \times F) + (15.2 \times \text{pH}) - (2711949 \times (d_{80}^2)) + (0.511 \times (F^2)) + (4.3 \times (\text{pH}^2)) - (50.195 \times d_{80} \times F) - (86.15 \times d_{80} \times \text{pH}) - (3.064 \times F \times \text{pH}) + (4.9 \times d_{80} \times F \times \text{pH}) \tag{19}$$

$$r^2 = 0.9422$$

$$\phi_c = 0.14 + (0.0423 \times (d_{80}^2)) - (1.935 \times 10^{-5} \times (F^2)) - (7.85 \times 10^{-5} \times (\text{pH}^2)) + (0.00981 \times d_{80} \times F) - (0.00215 \times d_{80} \times \text{pH}) + (0.0002056 \times F \times \text{pH}) + (0.000176 \times d_{80} \times F \times \text{pH}) \tag{20}$$

$$r^2 = 0.981$$

As mentioned in the Sect. 2, the batch flux density function, $f_{bk}(\phi)$, is a function of the solid volume fraction, ϕ , and can be obtained through using Eq. (2). Experimental methods for measurement of the parameters a and b have been explained by Rahimi et al. (2016a, b) and these parameters were determined at different conditions (pH, flocculant dosage and particle size).

According to experimental tests and using Curve expert professional software, parameters a , b were determined as a function of pH, flocculant dosage and particle size that are as follows:

$$a = 0.875 + (8.184 (d_{80}^2)) + (1.082 \times 10^{-4} \times (F^2)) - (1.51 \times 10^{-4} \times (\text{pH}^2)) - (0.0122 \times d_{80} \times F) + (0.0362 \times d_{80} \times \text{pH}) + (5.897 \times 10^{-4} \times F \times \text{pH}) - (0.00755 \times d_{80} \times F \times \text{pH})$$

$$r^2 = 0.947 \tag{21}$$

$$b = 91994.6 - (1069845 \times d_{80}) - (1.91 \times F) + (0.21 \times \text{pH}) + (2674630 \times (d_{80}^2)) + (0.03 \times (F^2)) + (0.014 \times (\text{pH}^2)) - (0.141 \times d_{80} \times F \times \text{pH})$$

$$r^2 = 0.975 \tag{22}$$

Table 1 compares the amount of parameters, a , b , n , ϕ_c and σ_0 that have been measured using experimental tests and have been predicted using model for input feed to tailing thickener of coal washing plant. It can be seen that there is a good agreement between the obtained results by experimental tests and the predicted results using model. Therefore, it is possible to predict amount of parameters a , b , n , ϕ_c and σ_0 using Eqs. (18) to (22) for tailing of coal washing plant.

4 Results and discussion

In this section, dynamic simulation of time dependent variation of pH for input feed to the thickener of coal washing plant is investigated. As mentioned before, Mathematical model of sedimentation and thickening [Eq. (1)] is complicated and does not have an analytical solution, but can be solved numerically using the finite difference method.

4.1 Constant particle size: $d_{80} = 275 \mu\text{m}$, constant flocculant dosage: $F = 40 \text{ g/t}$, First pH 9 and then pH 2

In order to simulate the time dependent variation of pH of input feed to tailing thickener of coal washing, the effective solid stress, the batch flux density function and the gel point were determined as a function of pH for input feed to the tailing thickener of coal washing plant that have been presented in the Sect. 3. Other parameters were obtained by direct measurement on the thickener unit. The parameters, which were used for simulation, have been shown in Table 2.

The flocculant dosage and particle size are constant at all times ($d_{80} = 275 \mu\text{m}$, $F = 40 \text{ g/t}$). The time-dependent variation of pH of input feed to thickener is as follows:

Table 1 Compare of parameters, a , b , n and φ_c that have been measured using experimental tests and have been predicted using model for input feed to tailing thickener of coal washing plant

No.	Particle size (d_{80}) (mm)	Flocculant dosage (F) (g/t)	pH	Parameter φ_c		Parameter n		Parameter a		Parameter b	
				Proposed by model	Actual	Proposed by model	Actual	Proposed by model	Actual	Proposed by model	Actual
1	0.275	40	9	0.299	0.298	5.77	5.78	1.075	1.16	16.78	18.89
2	0.275	40	6	0.274	0.273	5.34	5.51	1.22	1.18	20.17	19.87
3	0.275	40	2	0.24	0.241	4.76	4.01	1.43	1.46	25.09	24.2
4	0.275	20	9	0.223	0.231	3.8	3.78	1.27	1.2	25.96	23.55
5	0.275	20	6	0.2135	0.215	3.62	3.4	1.34	1.29	27.1	29
6	0.275	20	2	0.198	0.192	3.38	2.8	1.43	1.44	28.9	29
7	0.275	0	9	0.131	0.128	1.84	1.81	1.57	1.6	59.21	61
8	0.275	0	6	0.137	0.137	1.91	2.12	1.55	1.6	57.98	56
9	0.275	0	2	0.142	0.145	2	2.23	1.51	1.5	56.59	54.5
10	0.125	40	9	0.231	0.224	3.43	3.23	1.01	1	23.34	22
11	0.125	40	6	0.208	0.207	3.1	3.1	1.05	1	24.2	24
12	0.125	40	2	0.176	0.187	2.73	2.76	1.095	1.1	25.73	25.8
13	0.125	20	9	0.19	0.207	2.72	3.086	0.98	1	28.72	24.2
14	0.125	20	6	0.18	0.175	2.61	2.73	0.995	1.12	28.9	27
15	0.125	20	2	0.165	0.159	2.45	2.36	1	1	29	34
16	0.125	0	9	0.131	0.123	2	1.77	1.03	1	58.37	61.9
17	0.125	0	6	0.136	0.136	2.1	2.11	1.02	1	57.1	58.21
18	0.125	0	2	0.14	0.142	2.17	2.17	1.01	1	55.5	52

Table 2 Properties proposed to solve the model

Parameters	Conditions	Amount
Solid volume fraction of the thickener feed (φ_F)	All conditions	0.027
Feed flow rate (m^3/s)	All conditions	0.4651
Flow rate of thickener underflow (m^3/s)	All conditions	0.0358
Solid–fluid density difference ($\Delta\rho$) (kg/m^3)	All conditions	650
Acceleration of gravity (g) (m/s^2)	All conditions	9.81

$$pH = \begin{cases} 9 & 0 \leq t \leq 30000 \text{ s} \\ 2 & 30000 \text{ s} \leq t \leq 158000 \text{ s} \end{cases}$$

Figure 1 shows the simulation results of bed height and solid volume fraction of thickener underflow variations (response variables of simulation) at different times and pH values. Figure 2 shows the effect of pH variation on the response variables (solid volume fraction of thickener underflow and bed height) as a function of time.

As shown in the Figs. 1a and 2, with starting the thickening process, the pH value is 9 and solid volume fraction of thickener underflow and bed height increase with time. At $t = 3600$ s, the solid volume fraction of discharge and bed height are 0.263 and 1 m respectively and at $t = 30000$ s, the solid volume fraction of discharge

and bed height are 0.3175 and 1.7 m respectively. At $t = 30000$ s, amount of pH decreases from 9 to 2. With decreasing of pH value from 9 to 2, from $t = 30000$ s until $t = 32660$ s, the bed height is constant and solid volume fraction of discharge decreases from 0.3175 to 0.255.

From $t = 32660$ s, the bed height begin to increase slightly and solid volume fraction of discharge still decreases. It can be seen from Figs. 1b and 2 that with decreasing of pH from pH 9 to 2 and after 35760 s, solid volume fraction of discharge decreases from 0.3175 to 0.23 and bed height increases from 1.7 to 1.8. The time from $t = 30000$ s until $t = 35760$ s is transition period that pulp with the pH 9 and pulp with the pH 2 are in the thickener. After $t = 35760$ s, only the pulp with the pH 2 is in the thickener.

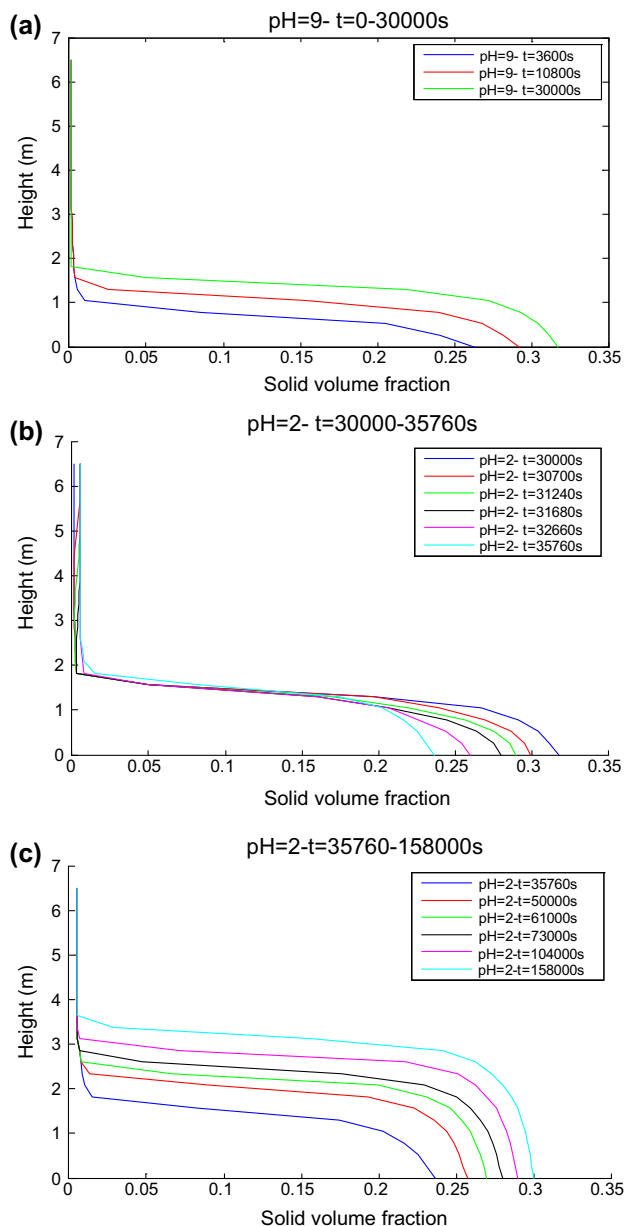


Fig. 1 The results of dynamic simulation of time-dependent variations of pH of input feed to thickener for the conditions: $d_{80} = 275 \mu\text{m}$, $F = 40 \text{ g/t}$, First pH 9 and then pH 2

The reasons that the solid volume fraction of discharge decreases from 0.3175 at $t = 30000 \text{ s}$ to 0.236 at $t = 35760 \text{ s}$ by decreasing of pH from 9 to 2, are as follows.

In our previous paper, it was concluded that in a certain amount of solid volume fraction, the effective solid stress increases with decreasing the pH in the case of flocculated suspension of the thickener of coal washing plant or in the certain amount of effective solid stress (certain amount of bed height), the solid volume fraction of discharge decreases with decreasing the pH (Rahimi et al. (2015)).

Therefore, in the certain amount of effective solid stress (certain amount of bed height), the solid volume fraction of discharge at pH 9 is higher than that at pH 2. In this research, after $t = 30000 \text{ s}$ at pH 9, bed height is 1.7 m and solid volume fraction of discharge is 0.3175. At $t = 30000 \text{ s}$, pH of flocculated suspension decreases from 9 to 2. In this bed height (1.7 m), the flocculated suspension has the solid volume fraction less than 0.3175 at pH 2. Therefore, at $t = 30000 \text{ s}$ and after decreasing amount of pH form 9 to 2, the solid volume fraction of discharge decreases and the bed height, first is constant and then increases slightly with increasing the time.

Figure 3 shows the results of dynamic simulation for the $d_{80} = 275 \mu\text{m}$, $F = 40 \text{ g/t}$ and constant pH 2 for all times. Other parameters are as the same as the parameters of Table 2.

It can be seen from Fig. 3 that when the amount of pH is constant and is equal 2, at $t = 13000 \text{ s}$, the solid volume fraction of discharge and bed height are 0.236 and 1.8 m, respectively. Therefore, it can be seen from the Figs. 1b and 2 that bed height increases slightly from 1.7 to 1.8 m and the solid volume fraction of discharge decreases with increasing the time to reach the solid volume fraction equivalent of bed height 1.8 m and at $t = 35760 \text{ s}$, the solid volume fraction of discharge is 0.236 that is solid volume fraction equivalent of bed height 1.8 m.

It can be seen form Figs. 1c and 2 that after $t = 35760 \text{ s}$, the solid volume fraction of discharge and bed height increase with increasing the time and at $t = 158000 \text{ s}$, the solid volume fraction of discharge and bed height are 0.3 and 3.4 m, respectively. With comparing the Figs. 1c and 3, it can be concluded that when the amount of pH is 2 and is constant for all time, the solid volume fraction of discharge and bed height are 0.3 and 3.4 m respectively, at $t = 135000 \text{ s}$. When the amount of pH is 9 and then decrease to 2, the solid volume fraction of discharge and bed height are 0.3 and 3.4 m respectively, at $t = 158000 \text{ s}$. Therefore, when the amount of pH is 2 and is constant for all time, the time to reach the mentioned conditions is less than when the amount of pH is 9 and then decrease to 2.

4.2 Constant particle size: $d_{80} = 275 \mu\text{m}$, Constant flocculant dosage: $F = 40 \text{ g/t}$, First pH 2 and then pH 9

The parameters which were used for simulation, have been shown in Table 2.

The flocculant dosage and particle size are constant at all times. In order to investigate the effect of time-dependent variations of pH of input feed to thickener, main parameters for all time are constant and time-dependent variations of pH of input feed to the thickener of coal washing plant are as follows:

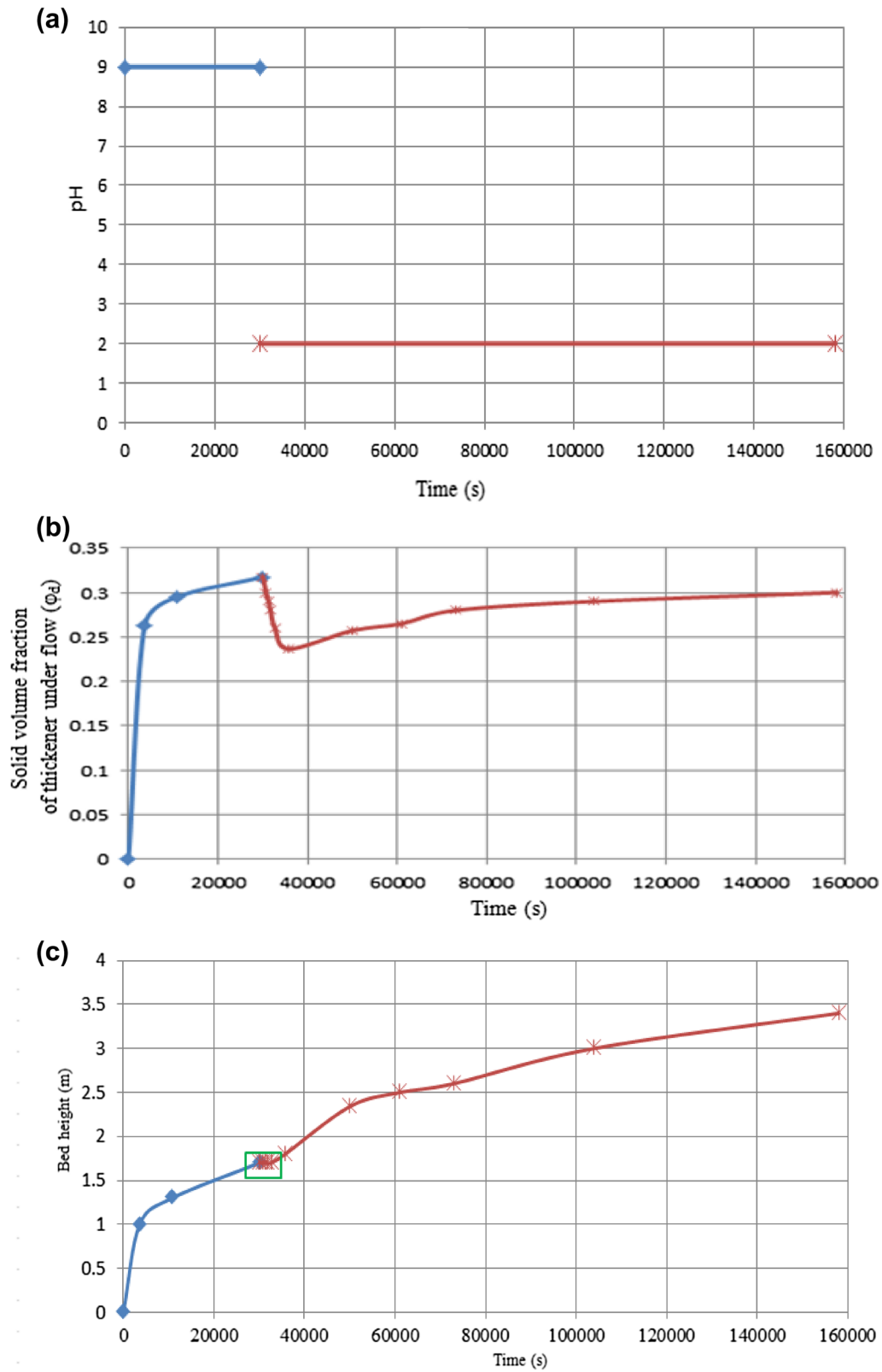


Fig. 2 The time-dependent variation of pH of input feed to thickener and simulation of changes of response variables for the conditions: $d_{80} = 275 \mu\text{m}$, $F = 40 \text{ g/t}$, First pH 9 and then pH 2

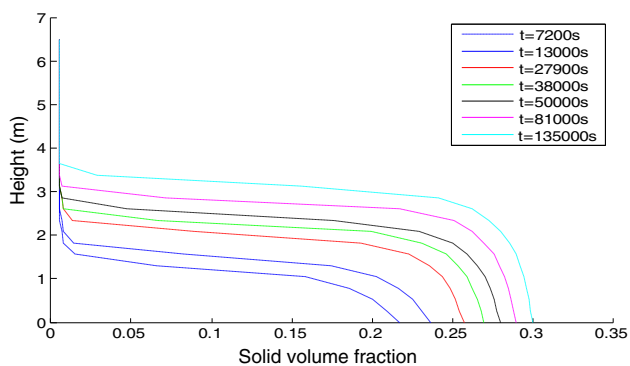


Fig. 3 Results of dynamic simulation for the $d_{80} = 275 \mu\text{m}$, $F = 40 \text{ g/t}$ and constant pH 2 ($Q_F = 0.465 \text{ m}^3/\text{s}$, $\varphi_F = 0.027$, $Q_D = 0.0358 \text{ m}^3/\text{s}$)

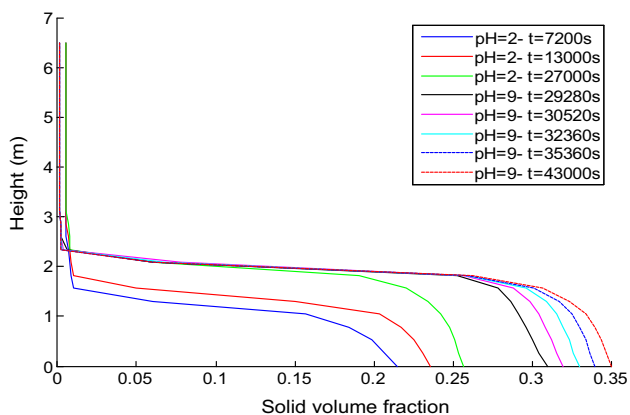


Fig. 4 Results of dynamic simulation of time-dependent variations of pH of input feed to the thickener of coal washing plant for the conditions: $d_{80} = 275 \mu\text{m}$, $F = 40 \text{ g/t}$, First pH 2 and then pH 9

$$\text{pH} = \begin{cases} 2 & 0 \leq t \leq 27000 \text{ s} \\ 9 & 27000 \text{ s} \leq t \leq 45000 \text{ s} \end{cases}$$

Figure 4 shows result of dynamic simulation for mentioned assumptions.

Figure 5 shows the time-dependent variations of pH of input feed to the thickener and simulation of change of response variables (solid volume fraction of thickener underflow and bed height) as a function of time.

As shown in the Figs. 4 and 5, with starting the thickening process, the pH value is 2 and solid volume fraction of thickener underflow and bed height increase with time. At $t = 7200 \text{ s}$, the solid volume fraction of discharge and bed height are 0.215 and 1.4 m respectively and at $t = 27000 \text{ s}$, the solid volume fraction of discharge and bed height are 0.256 and 2.2 m respectively. At $t = 27000 \text{ s}$,

amount of pH increases from 2 to 9. With increasing of pH value from 2 to 9, the bed height does not change and is constant but solid volume fraction of discharge will increase from 0.256 at high speed and pulp will reach to steady state condition at $t = 43000 \text{ s}$. The solid volume fraction of discharge is 0.35 at this time.

It was mentioned in the previous section that in a certain amount of solid volume fraction, the effective solid stress increases with decreasing the pH in the case of flocculated suspension of the thickener of coal washing plant or in the certain amount of effective solid stress (certain amount of bed height), the solid volume fraction of discharge decreases with decreasing the pH (Rahimi et al. (2015)).

Therefore, in the certain amount of effective solid stress or bed height, the solid volume fraction of discharge at pH 9 is higher than that at pH 2. In this research, after $t = 27000 \text{ s}$ at pH 2, the bed height is 2.2 m and solid volume fraction of discharge is 0.256. At $t = 27000 \text{ s}$ the pH of flocculated suspension increases from 2 to 9. In this bed height (2.2 m), the flocculated suspension has the solid volume fraction more than 0.256 at pH 9. Therefore, at $t = 27000 \text{ s}$ and after increasing the amount of pH form 2 to 9, the bed height is constant and solid volume fraction of discharge will increase at high speed with increasing the time to reach the solid volume fraction equivalent of bed height 2.2 m at pH 9.

Figure 6 shows the results of dynamic simulation for the $d_{80} = 275 \mu\text{m}$, $F = 40 \text{ g/t}$ and constant amount of pH 9 for all times. Other parameters are as the same as the parameters of Table 2.

It can be seen from Fig. 6 that when the amount of pH is constant and is equal 9, at $t = 135000 \text{ s}$, the pulp will reach to steady state condition and the solid volume fraction of discharge and the bed height are 0.35 and 2.2 m, respectively, at this time. After $t = 135000 \text{ s}$, the solid volume fraction of discharge and the bed height are constant and do not change.

With comparing the Figs. 4 and 6, it can be concluded that when the amount of pH is 9 and it is constant for all time, the solid volume fraction of discharge and bed height are 0.35 and 2.2 m respectively, at $t = 135000 \text{ s}$. When the amount of pH is 2 and then increase to 9, the solid volume fraction of discharge and bed height are 0.35 and 2.2 m respectively, at $t = 43000 \text{ s}$. Therefore, when the amount of pH is 9 and is constant for all time, the time to reach the mentioned conditions is higher than when the amount of pH is 2 and then increase to 9.

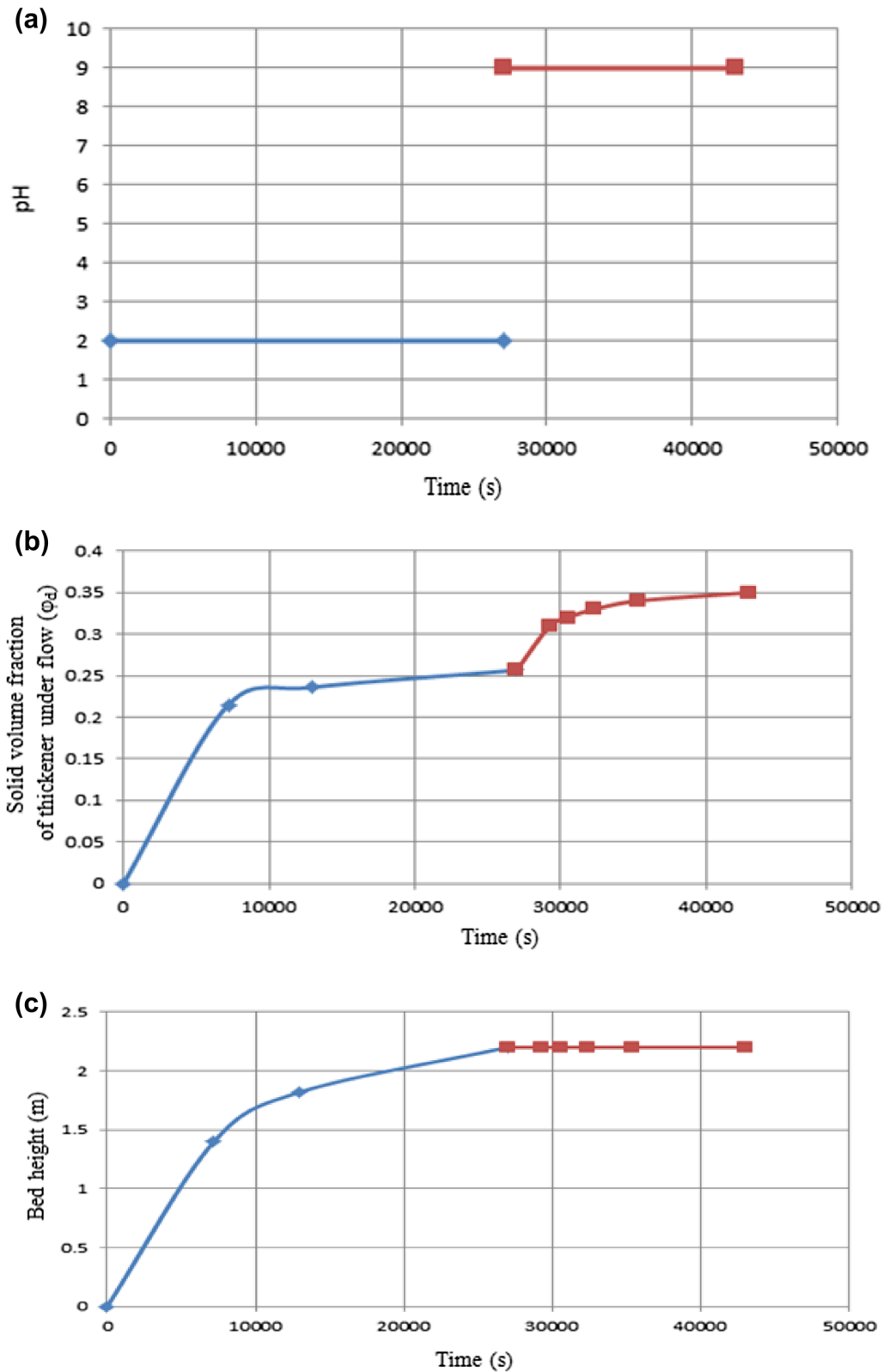


Fig. 5 The time-dependent variation of pH of input feed to the thickener and simulation of changes of response variables for the conditions: $d_{80} = 275 \mu\text{m}$, $F = 40 \text{ g/t}$, First pH 2 and then pH 9

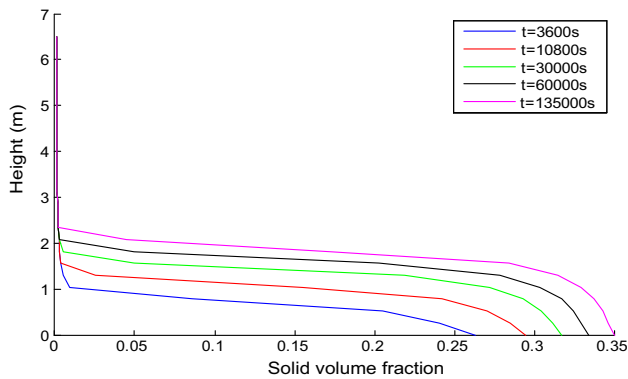


Fig. 6 Results of dynamic simulation for the $d_{80} = 275 \mu\text{m}$, $F = 40 \text{ g/t}$ and constant amount of pH 9 ($Q_F = 0.465 \text{ m}^3/\text{s}$, $\varphi_F = 0.027$, $Q_D = 0.0358 \text{ m}^3/\text{s}$)

5 Conclusion

It was mentioned that it is not possible to predict the thickener behavior as a function of time for time dependent variation of pH, flocculant dosage and particle size of input feed to thickener using phenomenological model of thickener in the Sect. 2, alone. Therefore:

- (1) The main parameters of phenomenological model of thickener (gel point, effective solid stress, batch flux density function) were determined as a function of particle size, pH and flocculant dosage of input feed to the thickener of coal washing plant using the results of experimental tests and Curve expert professional software. There is a good agreement between the obtained results by experimental tests and the predicted results using model. Therefore, it is possible to predict gel point, effective solid stress and batch flux density function using Eqs. (18–22) for tailing of coal washing plant.
- (2) It is possible to predict the thickener behavior as a function of time for time dependent variation of pH, flocculant dosage and particle size of input feed to the thickener of coal washing plant using obtained equations that it was not possible using phenomenological model of thickener alone.
- (3) The dynamic simulation was carried out for the industrial thickener of coal washing plant and the time-dependent variation of response variables (solid volume fraction of discharge and bed height) was investigated by time-dependent variation of pH of input feed to thickener using the obtained equations.

Open Access This article is distributed under the terms of the Creative Commons Attribution 4.0 International License (<http://creativecommons.org/licenses/by/4.0/>), which permits unrestricted use, distribution, and reproduction in any medium, provided you give appropriate credit to the original author(s) and the source, provide a

link to the Creative Commons license, and indicate if changes were made.

References

- Barth A, Burger R, Kroker I, Rohde C (2016) Computational uncertainty quantification for a clarifier-thickener model with several random perturbations: a hybrid stochastic Galerkin approach. *Comput Chem Eng* 89:11–26
- Burger R, Concha F (1998) Mathematical model and numerical simulation of the settling of flocculated suspensions. *Int J Multiphase Flow* 24:1005–1023
- Burger R, Bustos MC, Concha F (1999) Settling velocities of particulate systems: 9. Phenomenological theory of sedimentation processes: numerical simulation of the transient behavior of flocculated suspensions in an ideal batch or continuous thickener. *Int J Miner Process* 55:267–282
- Buscall R, White LR (1987) The consolidation of concentrated suspensions part I. The theory of sedimentation. *J Chem Soc Faraday Trans I* 83:873–891
- Garrido P, Burgos R, Concha F, Burger R (2004) Settling velocities of particulate systems: 13. A simulator for batch and continuous sedimentation of flocculated suspensions. *Int J Miner Process* 73:131–144
- Gladman BR, Rudman M, Scales PJ (2010) Experimental validation of a 1-D continuous thickening model using a pilot column. *Chem Eng Sci* 65:3937–3946
- Landman KA, White LR (1994) Solid/liquid separation of flocculated suspensions. *Adv Colloid Interface Sci* 51:175–246
- Landman KA, White LR, Buscall R (1988) The continuous-flow gravity thickener: steady state behavior. *AIChE J* 34:239–252
- Rahimi M, Abdollahzadeh A, Rezai B (2015) The effect of particle size, pH and flocculant dosage on the gel point, effective solid stress and thickener performance of coal washing plant. *Int J Coal Prep Util* 35:125–142
- Rahimi M, Abdollahzadeh A, Rezai B (2016a) Dynamic simulation of the effect of discharge rate variations on tailing thickener behavior of the coal-washing plant. *Int J Coal Prep Util* 36:91–108
- Rahimi M, Abdollahzadeh A, Rezai B (2016b) Dynamic simulation of tailing thickener at the Tabas coal washing plant using the phenomenological model. *Int J Miner Process* 154:35–40
- Rahimi M, Unesi M, Rezai B, Abdollahzadeh A (2017) Dynamic simulation of pilot thickener operation using phenomenological model with results validation for continuous and discontinuous tests. *J Cent South Univ* 24:1207–1216
- Richardson JF, Zaki WN (1954) The sedimentation of a suspension of uniform spheres under conditions of viscous flow. *Chem Eng Sci* 3(2):65–73
- Usher SP, Scales PJ (2005) Steady state thickener modeling from the compressive yield stress and hindered settling function. *Chem Eng J* 111:253–261
- Usher SP, Spehar R, Scales PJ (2009) Theoretical analysis of aggregate densification: impact on thickener performance. *Chem Eng J* 151:202–208
- Van Deventer BBG, Usher SP, Kumar A, Rudman M, Scales PJ (2011) Aggregate densification and batch settling. *Chem Eng J* 171:141–151
- Zhang Y, Martin A, Grassia P (2013) Mathematical modeling of time-dependent densified thickeners. *Chem Eng Sci* 2013(99):103–111
- Zhou T, Mao Li M, Li QL, Lei B, Chenn QZ, Zhou JM (2014) Numerical simulation of flow regions in red mud separation thickener's feedwell by analysis of residence-time distribution. *Trans Nonferrous Met Soc China* 24:1117–1124